Statistical Polarimetric RCS Model of an Asphalt Road Surface for mm-Wave Automotive Radar

Bouwmeester, Wietse; Fioranelli, Francesco; Yarovoy, Alexander

DOI
10.23919/EuRAD58043.2023.10289307

Publication date
2023

Document Version
Final published version

Published in
Proceedings of the 2023 20th European Radar Conference (EuRAD)

Statistical Polarimetric RCS Model of an Asphalt Road Surface for mm-Wave Automotive Radar

Wietse Bouwmeester, Francesco Fioranelli, Alexander Yarovoy
MS3 Group, Department of Microelectronics, Delft University of Technology, The Netherlands
{w.bouwmeester, f.fioranelli, a.yarovoy}@tudelft.nl

***Abstract* — A method for extracting fully polarimetric statistical properties of road surface radar cross sections is presented. This method is subsequently applied to extract radar cross section information from an asphalt road surface. Furthermore, an approach is introduced to synthesise the scattered signal of road surface returns as measured by a radar. The extracted statistical properties of asphalt are subsequently used in this synthesis procedure, and excellent agreement with the experimental measurement results is demonstrated.**

***Keywords* — polarimetry, radar, radar cross section, surface scattering, automotive.**

I. Introduction

Nowadays, an increasing amount of vehicles is being equipped with automotive radar systems that operate in the 77 GHz band to increase road safety. Compared to the previous generation of 24 GHz systems, modern automotive radar systems receive more intense backscattering from road surfaces due to the shorter wavelength. This drives the need for realistic radar cross section (RCS) models of road surfaces to increase accuracy of automotive radar simulation software, as well as for other applications such as determining antenna polarisation for road surface clutter rejection, or investigations of road surface condition classification. In previous works, measurements of road surface scattering at mm-wave frequencies have been presented [1]–[3]. However, literature on the statistical properties of road surface scattering or statistical models of the RCS of road surfaces is limited.

This paper presents a novel method to extract statistical RCS models from range profile measurement data. Additionally, an approach of synthesising road surface scattering is presented that allows to simulate road surface scattering in range, angle and Doppler domains. This method generates surface returns that show excellent agreement with measurement data. This synthesis method can subsequently be used to enhance the quality of simulation software.

The rest of the paper is organised as follows: section II presents the RCS model and the method for estimating the statistical properties of the normalised scattering parameters. Section III presents the measurement setup, with relevant results discussed in section IV. The proposed approach to synthesise road surface scattering is presented in section V and finally section VI concludes the paper.

II. Radar Cross Section Extraction

The first step in extracting the normalised scattering parameters of a surface-under-test (SUT) is to develop a model to compute the range profile as measured by radar systems. To this end, a surface is modelled as a grid of uncorrelated discrete scatterers. The distance, observation angles, and incidence angles relative to each scattering point can be computed using the equations outlined in [4]. Using the radar equation in (1), the ratio of returned power (P_x^{rx}) and transmitted power (P_y^{tx}) can be found for an individual scattering point. In (1), G_x^{rx} and G_y^{tx} are the antenna gains of the transmitting and receiving antennas, respectively, λ is the wavelength, A is the surface area of the scattering point and σ_{xy}^0 is its normalised RCS. Lastly, r represents the distance from the antenna to the surface scattering point. The x and y subscripts indicate the polarisation basis. For example, in this paper a horizontal/vertical polarisation basis is used, thus x and y can be either H or V. Furthermore, it should be noted that the gains, surface area, normalised RCS and range are dependent on the location of the scattering point.

$$\frac{P_x^{rx}}{P_y^{tx}} = \frac{G_x^{rx} G_y^{tx} \lambda^2 A \sigma_{xy}^0}{(4\pi)^3 r^4} = R_{xy} \sigma_{xy}^0 \tag{1}$$

Since the normalised scattering parameters are related to normalised RCS as

$$\sigma_{xy}^0 = \left| S_{xy}^0 \right|^2, \tag{2}$$

it can be seen that in conjunction with (1), the normalised scattering parameters can be determined from the measured complex-valued S-parameters S_{xy} as shown in (3).

$$S_{xy} = \frac{E_x^{rx}}{E_y^{rx}} = \sqrt{R_{xy}} S_{xy}^0 \tag{3}$$

This is possible as the returned power is related to half of the square of the magnitude of the returned electric field strength.

To compute the measured total scattering parameters as function of range, i.e. a range profile, the scattering parameters of the N scattering points within a range bin ρ are summed together, with each point indexed by i as shown in (4):

$$S_{xy}^{tot}(\rho) = \sum_{i=1}^{N} \sqrt{R_{xy,i}} S_{xy,i}^0. \tag{4}$$

Note that when the scattering from all points is uncorrelated, i.e. S_{xy}^0 has a random phase, $\left| S_{xy}^{tot} \right|^2$ and P_x^{rx}/P_y^{tx} converge towards the same value and thus power is conserved.

Using the model of measured range profiles, the statistical properties of the random variable S_{xy}^0 can be extracted. To do this, a few assumptions are made, namely:

- The normalised scattering parameters of the surface-under-test are isotropic, i.e. do not depend on azimuth of incident and reflected radiation.
- All scattering points of the surface-under-test within a range bin experience the same angle of incidence.

These assumptions ensure that within a range bin the equality $S^0_{xy,i} = S^0_{xy}$ holds.

As the first step, the extraction of $\langle S^0_{xy} \rangle$ from $\langle S^{tot}_{xy} \rangle$ is considered, where the angular brackets indicate the mean value of the statistical ensemble of scatterers. As

$$\begin{aligned} \langle S^{tot}_{xy}(\rho) \rangle &= \langle \sum_{i=1}^{N} \sqrt{R_{xy,i}} S^0_{xy} \rangle \\ &= \left(\sum_{i=1}^{N} \sqrt{R_{xy,i}} \right) \langle S^0_{xy} \rangle, \end{aligned} \tag{5}$$

the mean value of S^0_{xy} can be found using (6):

$$\langle S^0_{xy}(\rho) \rangle = \frac{1}{\sum_{i=1}^{N} \sqrt{R_{xy,i}}} \langle S^{tot}_{xy}(\rho) \rangle. \tag{6}$$

As each surface scattering point has a co- and cross-polar normalised scattering parameters for each of the two polarimetric channels which are not necessarily uncorrelated, the covariance of the normalised scattering parameters must also be found from the four measured range profiles. The covariance of S^0_{xy} and S^0_{uv} is related to the covariance of S_{xy} and S_{uv} via (7). Here, u & v are also indicators of the same polarisation basis as x & y but can differ from each other, to express all possible covariance permutations. In the equations, $Cov(A, B)$ is abbreviated to $C(A, B)$.

$$\begin{aligned} C\left(S^{tot}_{xy}, S^{tot}_{uv}\right) &= C\left(\sum_{i=1}^{N} \sqrt{R_{xy,i}} S^0_{xy}, \sum_{j=1}^{N} \sqrt{R_{uv,j}} S^0_{uv} \right) \\ &= \left(\sum_{i,j} \sqrt{R_{uv,i}} \sqrt{R_{xy,j}} \right) C\left(S^0_{xy}, S^0_{uv}\right) \end{aligned} \tag{7}$$

In (7), the sum over i and j represents all combinations of i and j. However, since the covariance of the normalised scattering parameters of scattering points i and j is 0 since the scattering points are uncorrelated, the covariance is found as:

$$C\left(S^{tot}_{xy}, S^{tot}_{uv}\right) = \left(\sum_{i=1}^{N} \sqrt{R_{uv,i}} \sqrt{R_{xy,i}} \right) C\left(S^0_{xy}, S^0_{uv}\right). \tag{8}$$

Therefore, the covariance of S^0_{xy} and S^0_{uv} can be found as:

$$C\left(S^0_{xy}, S^0_{uv}\right) = \frac{C\left(S^{tot}_{xy}, S^{tot}_{uv}\right)}{\sum_{i=1}^{N} \sqrt{R_{uv,i}} \sqrt{R_{xy,i}}}. \tag{9}$$

III. Experimental Measurements

To perform polarimetric measurements of road surface scattering, in this research a vector network analyser (VNA) of type N5242A was used together with frequency extenders to enable operation in the 75-85 GHz band. A SAR-1532-122-S2-DP dual-polarised horn antenna was used to collect polarimetric data and the entire measurement setup was mounted on a movable support designed to control the antenna orientation angle. The antenna orientation angle is defined as the angle in between the antenna boresight direction and the surface normal vector. More information on the measurement setup and settings can be found in [5]. The VNA was calibrated using a short-open-load-through procedure at the outputs of the frequency extenders. Then, to remove the effects of the differing channel lengths between the horizontally and vertically polarised channels of the antenna, measurements of a metal sphere were performed. As the scattering parameters of this canonical target are known, its measurements can be used to correct the phase error between the two polarimetric channels. To further remove measurement errors incurred by the antennas, a background measurement was taken by pointing the antenna at the sky. This could later be subtracted from the measurements of the SUT to enhance the sensitivity of the measurement setup.

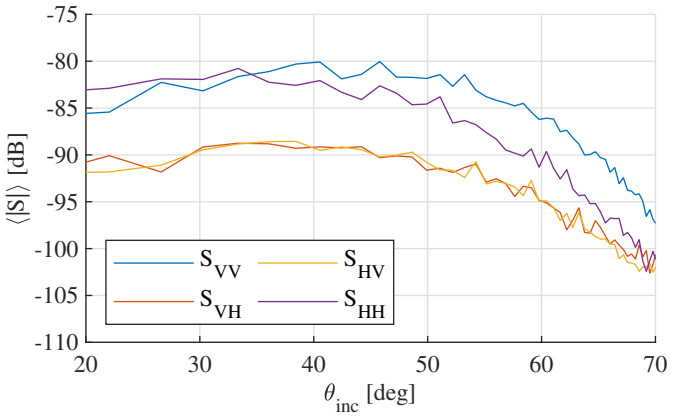

Fig. 1. Mean of magnitude of the scattering parameters of an asphalt road surface, measured with an antenna orientation angle of 60°.

After calibration, measurement data with antenna orientation angles of 60° and 90° was collected. Per antenna orientation angle, 50 measurements of a dry asphalt road surface were performed. To gather statistical surface scattering data, each measurement was performed at a position that was located a few centimetres apart from the previous measurements so that all measured patches of asphalt were geometrically uncorrelated as previous study showed that the correlation length of the surface roughness of asphalt is approximately 2 mm [5]. Finally, to obtain range-profile data from VNA frequency domain measurements, each measurement was transformed to time domain using inverse Fourier transforms.

IV. Experimental Results

Due to the geometry of the scenario, the angle of incidence is only dependent on the range and the height of the antenna, and thus the range axis can be translated to angle of incidence θ_{inc} using (10), where h is the height of the radar antenna and r the range.

$$\theta_{inc} = \arccos \frac{h}{r} \tag{10}$$

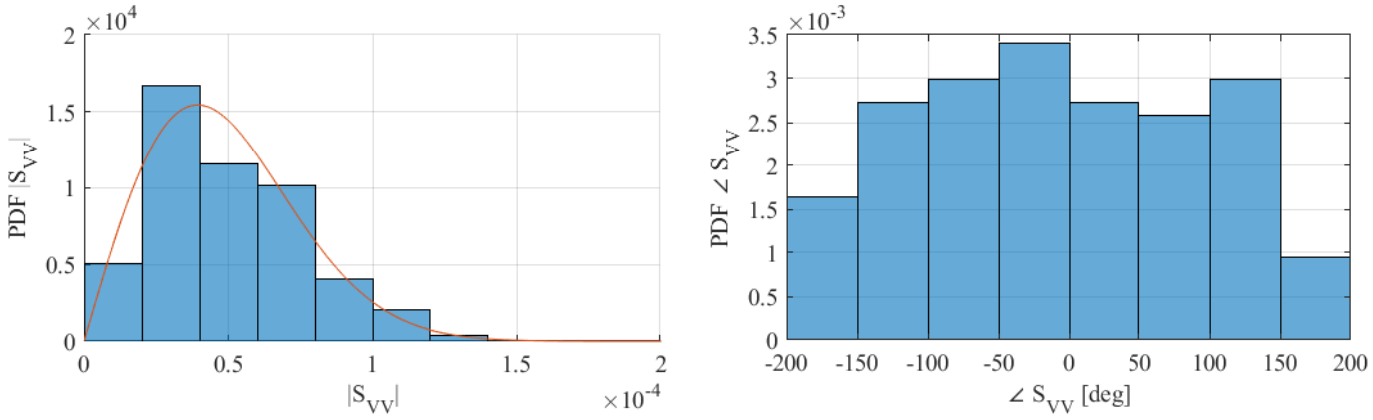

Fig. 2. Histograms normalised to represent the probability density functions of S_{VV} in the 59°-61° incident angle interval: (a) magnitude, compared to a Rayleigh distribution (in red) with the same variance as the measurement data; and (b) phase.

Fig. 1 shows the mean of the magnitude of the scattering parameters of the measured asphalt surface as a function of angle of incidence computed from the range-profiles using (10). The measurements in this plot were collected with an orientation angle of 60°. It can be seen that the maximum returned power takes place around 40° to 45°, which is some degrees below the antenna orientation angle of 60° at which the antenna gain is maximum. This is caused by the effect of propagation losses, as the surface area at 60° is slightly further away than the surface at 45°.

Subsequently, the distribution of the measured S-parameters can be investigated within an incident angle interval. Figs. 2a and 2b show the histograms created from the measured S_{VV} in the 59°-61° incident angle interval, normalised to represent the probability density function (PDF). Fig. 2a shows the PDF of the magnitude of S_{VV} and a comparison with a Rayleigh distribution of the same variance. Fig. 2b shows the PDF of the phase of S_{VV}. It can be seen that there is good correspondence between the Rayleigh distribution and the PDF of $|S_{VV}|$ and that the phase of S_{VV} approaches an uniform distribution. A similar observation is made for the other scattering parameters. This indicates that the real and imaginary components of the measured scattering parameters can be modelled as zero-mean normally distributed random variables.

As mentioned in section III, measurements were performed using both 60° and 90° antenna orientation angles. To maximise the signal to noise ratio of the surface scattering, the returned power from a surface with a normalised RCS of 1 is computed using the procedure presented in [4] for both 60° and 90° antenna orientation angles, and antenna gain patterns corresponding to those of the dual-polarised horn antenna used for the measurements. The range profiles of $|S_{VV}|$ for both antenna orientation angles are computed using (4), and shown in Fig. 3. As can be seen, at a range of approximately 1.45 m, the return from the 90° antenna orientation angle becomes stronger than the return from the 60° measurement. A similar analysis is performed for S_{VH} and S_{HH}, and where two of

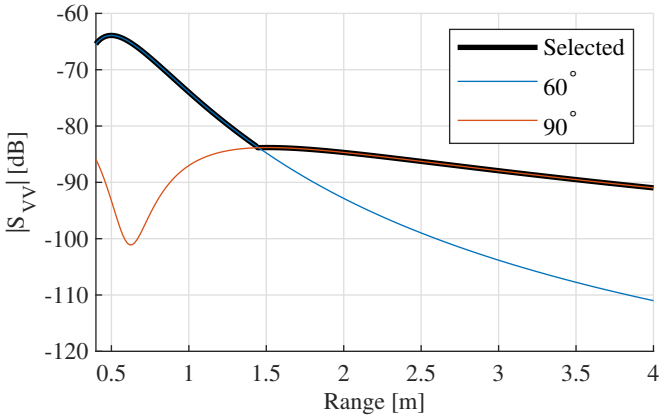

Fig. 3. Range profiles of S_{VV} for both 60° and 90° antenna orientation angles, where the normalised RCS of the surface is set to 1. The black line indicates the ranges where 60° or 90° where selected for RCS computation.

the three returns are strongest, measurements are selected for the corresponding antenna orientation angles to maximise the signal to noise ratio of the measured surface.

Finally, using the selected measurements, the mean values and covariance matrix of the normalised scattering parameters can be found using (6) and (9). From these, the expected value of the normalised RCS can be computed and is shown in Fig. 4.

V. Synthesis of Road Surface Scattering

As shown in section IV, the real and imaginary components of the measured scattering parameters are normally distributed random variables. Due to the central limit theorem, the normalised scattering parameters of each scattering point can also be modelled/simulated as normally distributed random variables. This is because when the contributions of each point are summed, normally distributed 'measured' scattering parameters result. Using this and the extracted normalised scattering parameters, range profiles can now be synthesised. This synthesis is not exclusively able to generate range

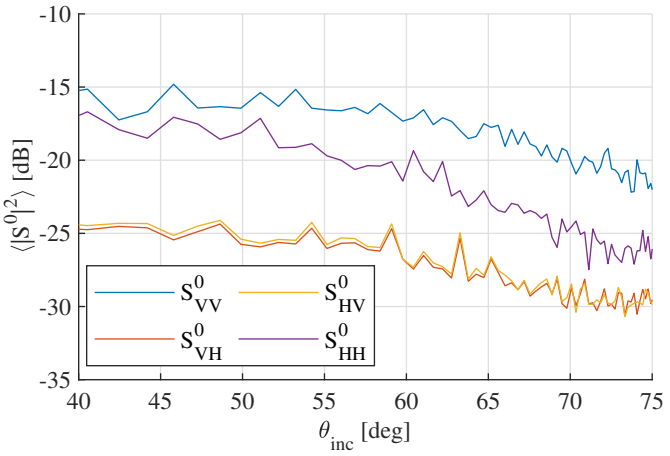

Fig. 4. Mean of the normalised radar cross section computed from the extracted mean and variance of the scattering parameters, computed from the combined range profiles of the asphalt surface measured with antenna orientation angles of 60° and 90°.

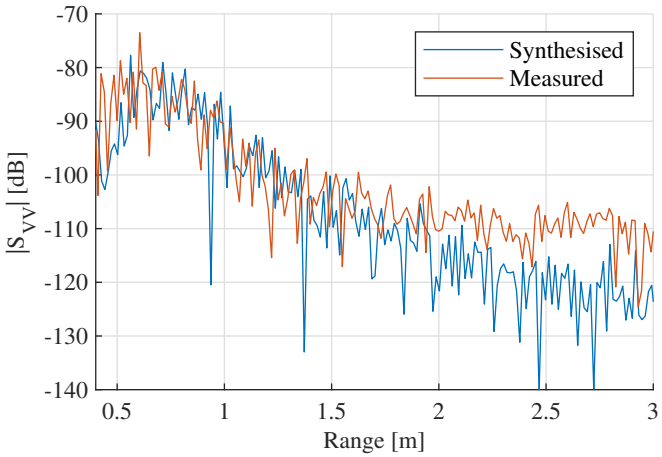

Fig. 5. Comparison of a synthesised range profile with a measured range profile recorded with an antenna orientation angle of 60°.

profiles, but can also be used to synthesise range-angle or range-Doppler profiles. The proposed synthesis comprises several steps:

1) Generate a grid of discrete scattering points.
2) Compute angle of incidence at each grid point.
3) Draw samples from a multivariate normal distribution for each point, with mean and covariance values as extracted for the correct incident angle.
4) Compute returned electric fields from scattering points.
5) Sum the returned fields in the correct range, angle and/or Doppler bin.

An example of results from this synthesis approach is shown in Fig. 5. Here, a comparison is made between a synthesised range profile and a measured range profile, acquired with an antenna orientation angle of 60°. It can be seen that there is excellent agreement within the 0.5 to 1.5 m interval, but there are deviations near the radar and from 1.5 m onwards. This is due to the limited sensitivity of the VNA, whose noise floor is located at around -110 dB. The deviations at close range are likely caused by reflections from parts of the measurement setup situated in a side lobe of the horn antenna.

VI. Conclusion

This paper presents a novel method of extracting polarimetric statistical properties of normalised scattering parameters, and by extension normalised RCS, from range profiles of rough surfaces. The method is based on an approach where the surface is modelled as a grid of point scatterers that each have normalised scattering coefficients following a multivariate distribution with a corresponding mean value and covariance matrix.

Subsequently, measurement results of range profiles of dry asphalt surfaces have been presented. From these results, it is shown that the real and imaginary components of the measured scattering parameters can be modelled by multivariate normal distributions.

Using the proposed method, the mean value and the covariance of the normalised scattering coefficients were extracted from measurement data. Using these values, plus the observation that the normalised scattering coefficients can also be modelled using a multivariate normal distribution, a method of synthesising responses was presented. The synthesised range profiles showed excellent correspondence to the measurement results at ranges where the measurement data was not limited by noise.

The developed RCS model and synthesis method can be used to simulate not only range profiles but also range-angle and/or range-Doppler profiles of road surfaces. This can be used for studies on classification of various road surface conditions. Furthermore, the proposed synthesis method can also be employed in general mm-wave automotive radar simulation software to increase accuracy of simulation results compared to the more simplistic models, such as the commonly used Lambertian model.

Acknowledgement

The authors thank F. van der Zwan for his help with the measurements.

References

[1] P. Asuzu and C. Thompson, "Road condition identification from millimeter-wave radar backscatter measurements," in *2018 IEEE Radar Conference (RadarConf18)*, Apr. 2018, pp. 0012–0016.

[2] K. Sarabandi, E. Li, and A. Nashashibi, "Modeling and measurements of scattering from road surfaces at millimeter-wave frequencies," *IEEE Transactions on Antennas and Propagation*, vol. 45, no. 11, pp. 1679–1688, Nov. 1997.

[3] M. Giallorenzo, X. Cai, A. Nashashibi, and K. Sarabandi, "Radar Backscatter Measurements of Road Surfaces at 77 GHz," in *2018 IEEE International Symposium on Antennas and Propagation & USNC/URSI National Radio Science Meeting*, Jul. 2018, pp. 2421–2422.

[4] W. Bouwmeester, F. Fioranelli, and A. Yarovoy, "Dynamic Road Surface Signatures in Automotive Scenarios," in *2021 18th European Radar Conference (EuRAD)*, Apr. 2022, pp. 285–288.

[5] ——, "Road Surface Conditions Identification via HαA Decomposition and Its Application to mm-Wave Automotive Radar," *IEEE Transactions on Radar Systems*, pp. 1–1, 2023. doi: 10.1109/TRS.2023.3286282